

1D NUMERICAL MODELING OF RESERVOIR SEDIMENTATION

By

Horacio Toniolo¹ and Gary Parker²

¹Assistant Professor, CEE Department, University of Alaska Fairbanks
P.O. Box: 755900 Fairbanks, AK 99775-5900
Phone: (907) 474 7977; Fax: (907) 474 6087; ffhat@uaf.edu

²Professor and Director of NCED, CE Department, University of Minnesota
Mississippi River at 3rd Ave. SE, Minneapolis, MN 55414
Phone: (612) 625-2397; Fax: (612) 624 4398; parke002@umn.edu

ABSTRACT

The depositional behavior of sand and mud in a reservoir is considered. Here the problem is simplified to sand-bed rivers that predominantly transport two grain sizes; sand as bed material load and mud as wash load. A sandy deltaic deposit is formed where a river reaches a reservoir. If the wash load is high enough to render the river water heavier than the reservoir water, the mud-laden river flow plunges to form a turbidity current. This mud is then deposited as a bottomset. The confinement of the reservoir can force the turbidity current to undergo an internal hydraulic jump, so forming an internal muddy pond downstream. The elevation of the top of the muddy pond may be below or above any outflow point. In the former case the trap efficiency of the reservoir is 100 percent; in the latter case it is less than 100 percent. The authors have previously developed and tested an integral, physically based, moving boundary model that captures the evolution of the river delta deposit, as well as the muddy deposit created by a ponded turbidity current. Here the model is applied to a hypothetical reservoir at field scale. The evolution of the location and elevation of the submerged hydraulic jump location is studied in this paper.

INTRODUCTION

All rivers transport sediment as well as water. Dam construction impacts the transport of both water and sediment. Because the great majority of rivers transport much more water than sediment a much longer time is required to fill a reservoir with sediment than with water. As a result the gradual accumulation of sediment in reservoirs often receives less attention that it merits. Sediment deposition in a reservoir reduces its storage capacity (Graf 1984; Fan and Morris 1992), so limiting the effective life of the dam as well as the benefits it provides. Sediment accumulation has been estimated to decrease worldwide reservoir storage by 1% per year (Mahmood 1987).

Sedimentation processes in reservoirs and lakes have been reported by many authors, i.e. Mahmood (1987), Hotchkiss and Parker (1991), Fan and Morris (1992), Sloff (1997), De Cesare et al. (2001), among many others. In recent years, experimental and numerical research on these topics has been actively pursued at Saint Anthony Falls Laboratory (SAFL), University of Minnesota. For instance, Kostic and Parker (2003a), (2003b) have developed a moving boundary model of deltaic sedimentation in lakes and reservoirs that captures the co-

evolution of the river-delta morphology and the associated deposit. Toniolo et al. (submitted (a)), (submitted (b)) have developed and tested an integral, physically based, moving boundary model that captures the evolution of the river-delta deposit, as well as the muddy lake deposit. The numerical model uses a shock-capturing technique that captures the location of any internal hydraulic jump dictated by the dam. This model was tested successfully against an experiment.

A field-scale simulation of the interaction between the prograding delta and the location of the internal hydraulic jump is presented in this paper.

FORMULATION

The analysis presented here represents a simplification of processes in reservoirs. A standing body of water is created in a river of constant width by means of a vertical barrier (dam). The river flow upstream of the barrier is Froude-subcritical and the barrier creates an M1 backwater curve. Sediments are characterized in terms of two grain sizes, i.e. size D_s in the sand range and size D_m in the mud (silt-clay) range. The sand (but no mud) deposits entirely in the topset and foreset of Figure 1. The mud is carried through the fluvial zone as wash load. The muddy water plunges in the vicinity of the foreset to form a purely depositional turbidity current that emplaces a bottomset composed purely of mud. Because of the assumption of a constant width the river flow upstream of the foreset is treated using the 1D St. Venant equations of shallow water flow, and the turbidity current downstream of the foreset is treated using the corresponding 1D layer-averaged relations for a turbidity current.

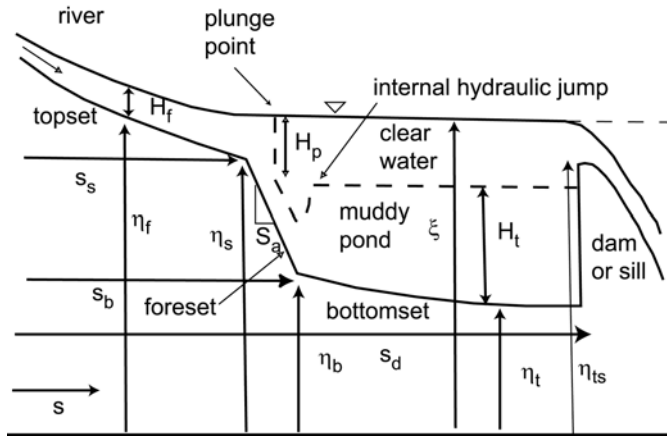
The 1D formulation of Toniolo et al. (submitted (a)) is briefly reviewed here. A definition diagram is given in Figure 1, in which s is a streamwise coordinate, $s = 0$ denotes the origin, s_s denotes the streamwise position of the topset-foreset break, s_p denotes the plunge point, s_b denotes the position of the foreset-bottomset break, and s_d denotes the position of the dam. Constant water discharge per unit width q_w , sand discharge per unit width q_{so} and mud discharge per unit width q_{mo} are supplied at $s = 0$.

The governing equations are transformed to hatted moving-boundary coordinates in order to capture the progradation of the delta. The fluvial zone extends from $s = 0$ to $s = s_s$, or $0 < \hat{s}_f < 1$. The equations to be solved over this zone are

$$\frac{dH_f}{d\hat{s}_f} = \frac{S_f - S_{fr}}{1 - \mathbf{Fr}^2} s_s \quad (1)$$

$$(1 - \lambda_{ps}) \left(\frac{\partial \eta_f}{\partial \hat{t}_f} - \hat{s}_f \frac{\dot{s}_s}{s_s} \frac{\partial \eta_f}{\partial \hat{s}_f} \right) = - \frac{1}{s_s} \frac{\partial q_s}{\partial \hat{s}_f} \quad (2)$$

where η_f denotes bed elevation, H_f denotes flow depth, S_f denotes bed slope, S_{fr} denotes friction slope which is in turn related to a bed friction coefficient C_{fa} , \mathbf{Fr} denotes the Froude number of open-channel flow, \hat{t}_f denotes time on the fluvial zone, q_s denotes the volume transport of sand per unit width and λ_{ps} denotes the porosity of fluvial deposits of sand. Here C_{fa} is specified as the ratio $\tau_b/(\rho U^2)$ where τ_b denotes boundary shear stress at the bed, ρ denotes water density and U denotes depth-averaged flow velocity. A generalized sediment transport relation of the following form is assumed for the bed-material transport of sand;



$$q^* = \alpha(\tau^* - \tau_c^*)^n \quad (3a)$$

where α and n are specified parameters, q^* and τ^* are defined as

$$q^* = \frac{q_s}{\sqrt{R_s g D_s D_s}} \quad (3b,c)$$

$$\tau^* = \frac{\tau_b}{\rho R_s g D_s}$$

and R_s denotes the submerged specific gravity of sand (about 1.65 for natural quartz) and g = the acceleration of gravity.

Figure 1. Sketch of geometric configuration considered in the formulation. The flow is from left to right.

In addition, the parameter τ_c^* in Eq. (3a) denotes a critical Shields stress for the onset of sand motion. The total bed material load relation of Engelund and Hansen (1972) used here is realized for the choices

$$\alpha = \frac{0.05}{C_{fa}} \quad n = 2.5 \quad \tau_c^* = 0 \quad (4a,b,c)$$

The boundary conditions on Eqs. (1) and (2) are

$$q_s|_{\hat{s}_f=0} = q_{so} \quad H_f|_{\hat{s}_f=l} = \xi - \eta_s \quad (5a,b)$$

where q_{so} denotes a specified constant sediment feed rate, ξ denotes the constant water surface elevation of the reservoir and η_s denotes the bed elevation at the topset-foreset break. Progradation of the topset-foreset break is specified in terms of a shock condition;

$$\dot{s}_s = \frac{1}{S_a} \left[-\frac{\partial \eta_f}{\partial \hat{t}_f} \Big|_{\hat{s}_f=l} + \frac{1}{s_b - s_s} \frac{q_{ss}}{(1 - \lambda_{ps})} \right] \quad (6)$$

where \dot{s}_s denotes the speed of migration of the topset-foreset break, S_a denotes the specified foreset slope and q_{ss} denotes the value of q_s at the topset-foreset break. Progradation of the foreset-bottomset break is specified in terms of a continuity condition;

$$\dot{s}_b = \dot{s}_s + \frac{1}{S_a} \left(\frac{\partial \eta_f}{\partial \hat{t}_f} \Big|_{\hat{s}_f=l} - \frac{\partial \eta_t}{\partial \hat{t}_t} \Big|_{\hat{s}_t=0} \right) \quad (7)$$

where \dot{s}_b denotes the speed of migration of the foreset-bottomset break, \hat{s}_t denotes a moving-boundary coordinate along the bottomset such that $\hat{s}_t = 0$ denotes the position of the foreset-bottomset break, $\hat{s}_t = l$ denotes the position of the dam, \hat{t}_t denotes time on the turbidity current zone and η_t denotes bottomset bed elevation.

Plunging occurs on the face of the foreset, and is computed using the method of Parker and Toniolo (submitted), which is in turn based on that of Akiyama and Stefan (1984). The turbidity current dynamics are described by the relations

$$\begin{aligned}
 \frac{\partial H_t}{\partial \hat{t}_t} - \frac{\dot{s}_b(1-\hat{s}_t)}{s_d-s_b} \frac{\partial H_t}{\partial \hat{s}_t} + \frac{1}{s_d-s_b} \frac{\partial U_t H_t}{\partial \hat{s}_t} &= (1-\delta)e_w U_t - \delta v_{sm} \\
 \frac{\partial C_t H_t}{\partial \hat{t}_t} - \frac{\dot{s}_b(1-\hat{s}_t)}{s_d-s_b} \frac{\partial C_t H_t}{\partial \hat{s}_t} + \frac{1}{s_d-s_b} \frac{\partial U_t C_t H_t}{\partial \hat{s}_t} &= -r_o v_{sm} C_t \\
 \frac{\partial U_t H_t}{\partial \hat{t}_t} - \frac{\dot{s}_b(1-\hat{s}_t)}{s_d-s_b} \frac{\partial U_t^2 H_t}{\partial \hat{s}_t} + \frac{1}{s_d-s_b} \frac{\partial U_t^2 H_t}{\partial \hat{s}_t} + \delta U_t v_{sm} &= \\
 -\frac{1}{2} \frac{R_m g}{s_d-s_b} \frac{\partial C_t H_t^2}{\partial \hat{s}_t} + R_m g C_t H_t S_t - C_{fs} U_t^2 &
 \end{aligned} \tag{8,9,10}$$

where H_t , U_t and C_t denotes turbidity current thickness, velocity and volume concentration of sediment, v_{sm} denotes the fall velocity of the mud calculated from the relation of Dietrich (1982), e_w is a coefficient of entrainment of ambient water into the turbidity current, a relation for which given in Parker et al. (1986), r_o is an order-one coefficient here set to unity, R_m denotes the submerged specific gravity of the mud, C_{fs} denotes a bottom friction coefficient of the turbidity current and δ is equal to 1 in the ponded zone and 0 otherwise. More specifically, the term δv_{sm} in Eq. (8) plays the essential role of describing detrainment of water across a settling interface, and thus serves to allow the possibility for the top of the ponded turbidity current to equilibrate at a point below any point of outflow from the reservoir.

For dilute turbidity currents, the characteristic time for significant migration of the foreset-bottomset break is much larger than the setup time for quasi-steady flow with an internal hydraulic jump. Equivalently, this implies that $\dot{s}_b/U_t \ll 1$, i.e., the speed of a slow-moving ponded turbidity current is still much faster than the speed of delta progradation. As a result, Eqs. (8,9,10) can be accurately approximated to

$$\begin{aligned}
 \frac{\partial H_t}{\partial \hat{t}_t} + \frac{1}{s_d-s_b} \frac{\partial U_t H_t}{\partial \hat{s}_t} &= (1-\delta)e_w U_t - \delta v_{sm} \\
 \frac{\partial C_t H_t}{\partial \hat{t}_t} + \frac{1}{s_d-s_b} \frac{\partial U_t C_t H_t}{\partial \hat{s}_t} &= -r_o v_{sm} C_t \\
 \frac{\partial U_t H_t}{\partial \hat{t}_t} + \frac{1}{s_d-s_b} \frac{\partial U_t^2 H_t}{\partial \hat{s}_t} + \delta U_t v_{sm} &= \\
 -\frac{1}{2} \frac{R_m g}{s_d-s_b} \frac{\partial C_t H_t^2}{\partial \hat{s}_t} + R_m g C_t H_t S_t - C_{fs} U_t^2 &
 \end{aligned} \tag{11,12,13}$$

The upstream boundary conditions on Eqs. (11), (12) and (13) take the form

$$H_t|_{s_p} = H_d \quad U_t|_{s_p} = U_d \quad C_t|_{s_p} = C_d \tag{14,15,16}$$

where H_d , U_d and C_d denote the thickness, layer-averaged velocity and volume concentration of the turbidity current just downstream of plunging. The values of H_d , U_d and C_d are computed using the formulation of plunging of Parker and Toniolo (submitted), which requires the specification of a single mixing coefficient γ , where

$$U_d H_d = (1+\gamma)q_w \tag{17}$$

This parameter characterizes the degree to which plunging entrains ambient clear water from the upper layers of the reservoir into the turbid underflow.

The turbidity current is allowed to run down the foreset without depositing sediment until it reaches the foreset-bottomset break, at which $\hat{s}_t = 0$. Beyond this point the bed is allowed to evolve according to the relation

$$(1 - \lambda_{pm}) \left(\frac{\partial \eta_t}{\partial \hat{t}_t} - \frac{\dot{s}_b (1 - \hat{s}_t)}{s_d - s_b} \frac{\partial \eta_t}{\partial \hat{s}_t} \right) = r_o C_t \quad (18)$$

which describes a purely depositional turbidity current. In the above relation, λ_{pm} denotes the porosity of the mud deposit.

The nature of the boundary condition at the dam changes depending on whether the elevation of the settling interface in the ponded zone, ξ_{mp} , is below or above an outflow sill, as described in Figure 1. In the present work, however, the condition of no overflow is considered. The downstream boundary condition at the dam for this case is simply

$$U_t|_{s=s_d} = U_t|_{\hat{s}_t=1} = 0 \quad (19)$$

IMPLEMENTATION OF THE NUMERICAL MODEL

A detailed description of the numerical implementation of the above formulation is given in Toniolo et al. (submitted (b)). However, a summary of the solution technique is given here. The upstream values of the volume transport rates of sand and mud per unit width, q_{so} and q_{mo} , respectively are specified, along with the water surface elevation ξ , the slope S_a of the avalanching foreset, the water discharge q_w , distance to the dam barrier s_d and the parameters D_s , D_m , R_s , R_m , λ_{ps} , λ_{pm} , C_{fa} , C_{fs} and r_o . At any given time the bed profile, and thus the values (η_s, s_s) and (η_b, s_b) are known. Eq. (1) is then solved numerically upstream subject to Eq. (5b) to determine the depth profile on the fluvial zone. The depth profile combined with Eqs. (3b), (3c) allows an evaluation of the sand transport rate q_s everywhere on the fluvial zone. The speed of migration of the topset-foreset break \dot{s}_s is then evaluated from Eq. (4). The bed profile on the fluvial zone one time step later is then obtained from a numerical solution of Eq. (2) subject to Eq. (5a). The time step used to discretize Eq. (2) is here called a morphologic time step, as it is the one that characterizes bed change in time. In principle the above method would also use a much shorter hydraulic time step to compute the time progress of the flow toward quasi-steady conditions, but the quasi-steady assumption obviates this.

The turbidity current zone is solved rather differently, using the same morphologic time step as that used in the fluvial region, as well as a much shorter hydraulic time step. The temporal terms in Eqs. (11,12,13) are used as a way of iterating in hydraulic time toward a quasi-steady solution that nevertheless automatically captures any internal hydraulic jump. The MacCormack scheme (MacCormack 1969; Tannehill et al. 1997) is used to solve the Eqs. in this submodel. This scheme is second order accurate in both space and time. Details of the numerical implementation of this submodel are presented in Toniolo et al. (submitted (c)).

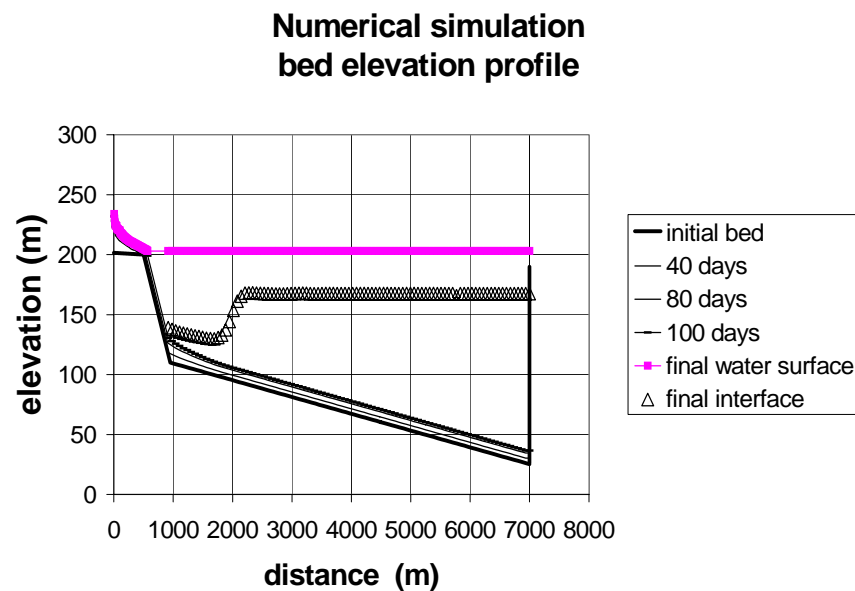
Consider a case for which the turbidity current is suddenly released from the plunge point at time $t = 0$. The turbidity current will run down the plunge point, across the bottomset and up the barrier of the dam. It will then reflect and send a bore migrating upstream, which will eventually stabilize as an internal hydraulic jump. Once this relatively short setup period is passed, the resulting flow is quasi-steady, in that the bed and flow change only in response to

the slow process of sediment deposition. Implicit in the above arguments are two time scales, one hydraulic and one morphologic, that differ greatly from each other.

Thus at any given time step an appropriate (but rather arbitrary) initial condition is applied for the turbidity current calculation, and Eqs. (11,12,13) are solved according to the upstream boundary conditions of (14,15,16). Eq. (19) defines the downstream boundary condition. The calculation is continued in hydraulic time until a quasi-steady condition is reached. Only this quasi-steady solution is used in evaluating the bed change. In particular, it is used in Eqs. (18) and (5) to evaluate the change in bottomset bed elevation and the migration speed \dot{s}_b of the foreset-bottomset break.

FIELD-SCALE NUMERICAL SIMULATION

Toniolo et al. (submitted (b)) successfully tested the numerical model against a laboratory experiment conducted at SAFL. In the present work, the numerical model is applied to a hypothetical reservoir at field scale. A condition of no overflow is fixed at the downstream end. The geometrical conditions are summarized in Figure 1.

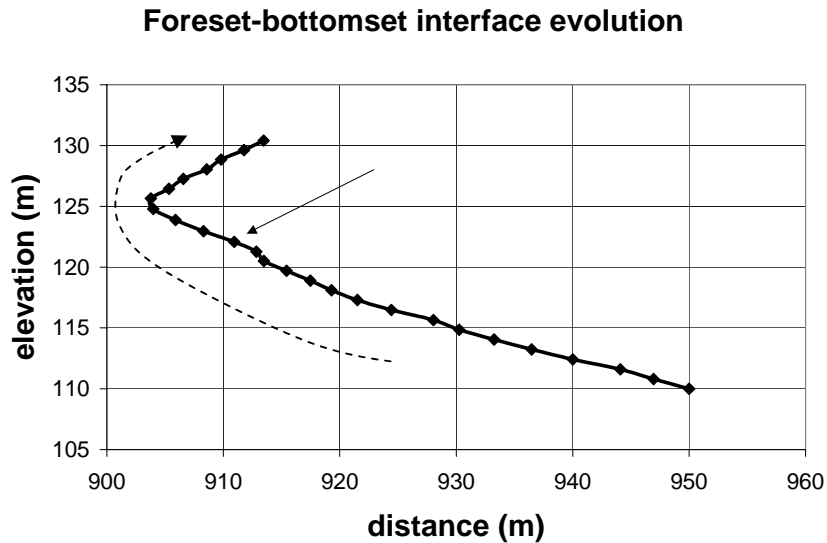


More specifically, they are as follows: the length $s_d = 7000$ m and the initial length of fluvial zone $s_{si} = 500$ m. The initial topset and bottomset bed slopes S_{fi} and S_{ti} are 0.003 and 0.014 respectively. The initial elevations of the top and bottom of the foreset η_s and η_b are 200 m and 110 m, respectively. The foreset slope S_a is set equal to 0.2 (11.3°).

Figure 2. Bed elevation profile in function of time. The turbidity current interface after 100 days is also included in the graph. The internal hydraulic jump and ponded turbidity current can be clearly seen in the plot.

The water surface elevation in the reservoir is fixed at 203 m. Neither orifices nor gates are considered at the downstream end. The specific water discharge q_w of the river is set to $2.2 \text{ m}^2/\text{s}$. The mixing coefficient γ at the plunging point is 0.9. The dimensionless Chezy resistance coefficients $C_{fa}^{-1/2}$ and $C_{fs}^{-1/2}$ for the subaerial (topset) and subaqueous (bottomset) regimes are set equal to 12 and 30 respectively. The simulation uses sand with $D_s = 400 \text{ }\mu\text{m}$, $R_s = 1.65$, and $\lambda_{ps} = 0.4$ and mud with $D_s = 50 \text{ }\mu\text{m}$, $R_s = 1.65$, and $\lambda_{pm} = 0.55$. The input rates

q_{so} and q_{mo} of sand and mud are $7.25 \times 10^{-4} \text{ m}^2/\text{s}$ and $3.00 \times 10^{-3} \text{ m}^2/\text{s}$, respectively. The ratio between sand and total input rate $q_{so}/(q_{so} + q_{mo})$ is 0.195.



The total run time is 100 days of continuous flood flow, which easily translates into years or decades of real time. The geomorphic time step, i.e. that used in Eqs. (2) and (13), is taken to be 2 h. The fluvial and subaqueous regions are divided into 94 nodes each.

Figure 3. Foreset-bottomset interface evolution. The competition between the sand deposit on the foreset and the mud deposit from the turbidity current is clearly shown in the graph. The dashed arrow denotes the progress of time. The solid arrow indicates the interface position at which the jump moves downstream.

Figure 2 illustrates the evolution of the bed profile in time. The final profile of the turbidity current interface showing the submerged hydraulic jump and the ponded zone is included. The gradual filling of the reservoir as the foreset progrades and the bottomset builds up is clearly documented.

Figure 3 shows the evolution in time of the foreset-bottomset interface. Each dot in the graph represents a time interval of 4 days. The foreset-bottomset interface moves upstream until the bed sediment from the river builds a prograding delta with sufficient velocity that moves the interface downstream. Figure 4 documents the same deposition pattern along the Colorado River through Lake Mead, 1935-1948.

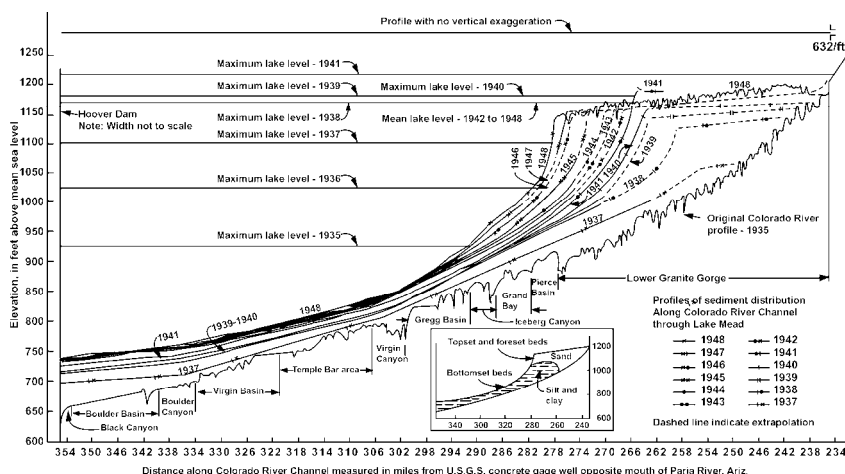


Figure 4. Deposition pattern along the Colorado River through Lake Mead, 1935 – 1948. From Graf (1984), based on an original in Grover and Howard (1937). The flow is from right to left.

Figures 5 and 6 show the variation of jump location in time and the bed elevation where the jump was located, respectively. According to Figure 5, the hydraulic jump was located between 1800 and 2000 m from the origin. Figure 5 indicates the jump moved upstream during an initial period of 60 days, with a sudden displacement after 28 days. This tendency

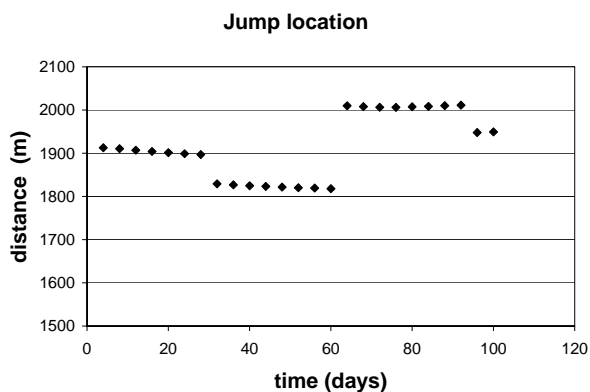


Figure 5. Submerged hydraulic jump location.

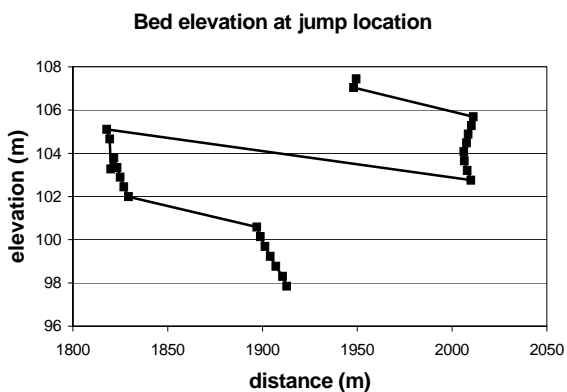


Figure 6. Bed elevation at jump location.

was subsequently reversed at 60 days, with a sudden downstream movement of approximately 200 m (solid arrow in Figure 3). Figure 6 shows the bed elevation associated with these displacements. The interaction between water entrainment, sediment deposition in the supercritical region and water detrainment in the ponded zone apparently caused these changes in the position of the submerged hydraulic jump.

CONCLUSIONS

The numerical model presented in Toniolo et al. (submitted (a), submitted (b)) represents an important step toward a numerical model capable of predicting reservoir trap efficiency. It captures the sand-mud evolution in deltas. It is the first model that can track both turbidity current regimes in the reservoir, i.e. supercritical and subcritical. Also, it captures the

mechanics of an important phenomenon in reservoir sedimentation: formation of an internal muddy pond downstream of an internal hydraulic jump.

A condition of no overflow at the downstream end of the reservoir (sediment trap efficiency of 100 percent) was used here to show the time variation of the jump location. The model is easily amended to describe the rise of the interface of the muddy pond to a point at which sediment starts escaping from the reservoir (Toniolo et al., submitted (b)).

REFERENCES

- Akiyama, J., and Stefan, H. (1984). "Plunging flow into a reservoir: Theory." *Journal of Hydraulic Engineering*, ASCE, 110(4), 484-499.
- De Cesare, G., Schleiss, A., and Hermann, F. (2001). "Impact of Turbidity Currents on Reservoir Sedimentation." *Journal of Hydraulic Engineering*, ASCE, 127(1), 6-16.
- Dietrich, E.W. (1982). "Settling velocities of natural particles." *Water Resources Research*, 18 (6), 1626 – 1682.
- Engelund, F., and Hansen, E. (1972). "A monograph on sediment transport." Technisk Forlag, Copenhagen, Denmark.
- Fan, J., and Morris, G. (1992). "Reservoir sedimentation. I: Delta and density current deposits." *Journal of Hydraulic Engineering*, ASCE, 118(3), 354-369.
- Graf, W. H. (1984). "Hydraulics of sediment transport." McGraw-Hill, New York, 513 p.
- Grover, N., and Howard, C. (1937). "The Passage of Turbid Water Through Lake Mead." *Trans. ASCE* 103, 720-790.
- Hotchkiss, R. H., and Parker, G. (1991). "Shock fitting of aggradational profiles due to backwater." *Journal of Hydraulic Engineering*, 117(9), 1129-1144.
- Kostic, S., and Parker, G. (2003a). "Progradational sand-mud deltas in lakes and reservoirs. Part 1: Theory and numerical model." *Journal of Hydraulic Research*, 41(2).
- Kostic, S., and Parker, G. (2003b). "Progradational sand-mud deltas in lakes and reservoirs. Part 2. Experiment and numerical simulation." *Journal of Hydraulic Research*, 41(2).
- MacCormack, R. (1969). "The effect of viscosity in hypervelocity impact cratering." *Paper* 69-354, American Institute of Aeronautics and Astronautics, Cincinnati, Ohio.
- Mahmood, K. (1987). "Reservoir sedimentation: Impact, extent and mitigation." *Technical paper* No.71, The World Bank, Washington D.C.
- Parker, G., Fukushima, Y., and Pantin, H. M. (1986). "Self-accelerating turbidity currents." *Journal of Fluid Mechanics* 171, 145-181.

- Parker, G., and Toniolo, H. (submitted). "A note on the analysis of plunging density flows." *Journal of Hydraulic Engineering*, ASCE.
- Sloff, C.J. (1997). "Sedimentation in reservoirs." *Ph.D. Thesis*, Technical University of Delft, the Netherlands, 269 p.
- Tannehill, J., Anderson, D., and Pletcher, R. (1997). "Computational Fluid Mechanics and Heat Transfer". Second edition. Taylor & Francis, Washington DC, 792 p.
- Toniolo, H., Parker, G., and Voller, V. (submitted (a)). "Role of ponded turbidity currents in reservoir trap efficiency: formulation." *Journal of Hydraulic Engineering*.
- Toniolo, H., Parker, G., and Voller, V. (submitted (b)). "Role of ponded turbidity currents in reservoir trap efficiency: experiment and simulation." *Journal of Hydraulic Engineering*.
- Toniolo, H., Parker, G., and Voller, V. (submitted (c)). "Depositional turbidity currents in diapiric minibasins on the continental slope: experiments and numerical simulation." *Journal of Sedimentary Research*.
- de Vries, M. (1965). Consideration about non-steady bed-load-transport in open channels. Proc. IAHR, 11th Congress, Vol. 3, Paper 3.8, 11p.